

Effective interaction for relativistic mean-field theories of nuclear structure

H. B. Ai, L. S. Celenza, A. Harindranath, and C. M. Shakin

Department of Physics and Center for Nuclear Theory, Brooklyn College of the City University of New York, Brooklyn, New York 11210

(Received 16 October 1986)

We construct an effective interaction, which when treated in a relativistic Hartree-Fock approximation, reproduces rather accurately the nucleon self-energy in nuclear matter and the Migdal parameters obtained via relativistic Brueckner-Hartree-Fock calculations. This effective interaction is constructed by adding Born terms, describing the exchange of pseudoparticles, to the Born terms of the Dirac-Hartree-Fock analysis. The pseudoparticles have relatively large masses and either real or imaginary coupling constants. (For example, exchange of a pseudo-sigma with an imaginary coupling constant has the effect of *reducing* the scalar attraction arising from sigma exchange while exchange of a pseudo-omega with an imaginary coupling constant has the effect of *reducing* the repulsion arising from omega exchange. The terms beyond the Born term in the case of pion exchange are well simulated by pseudo-sigma exchange with a *real* coupling constant.) The effective interaction constructed here may be used for calculations of the properties of finite nuclei in a relativistic Hartree-Fock approximation.

I. INTRODUCTION

The description of nuclear matter as a relativistic system has led to a good understanding of various nuclear properties.¹⁻³ Further, the use of the relativistic impulse approximation has been quite successful in describing nucleon-nucleus scattering.⁴ A natural extension of the relativistic analysis lies in the study of the structure of finite nuclei. While it is possible to describe finite nuclei using either a mean-field (Dirac-Hartree) approach⁵ or a Dirac-Hartree-Fock analysis,⁶ such calculations involve the introduction of a number of free parameters. The *phenomenological* theories, such as the relativistic Brueckner-Hartree-Fock theory^{1,2} or the relativistic impulse approximation,⁴ are parameter free. We would like to describe the properties of finite nuclei using the parameter-free (phenomenological) approach. To that end one might contemplate the calculation of relativistic Brueckner reaction matrices for a finite system. That is a very difficult program and we do not attempt such calculations. We are here interested in obtaining an effective interaction which may be used in a (Dirac) Hartree-Fock approximation for the study of finite nuclei. The interaction should be "realistic" in the sense that matrix elements of the effective interaction should reproduce the matrix elements calculated with the reaction matrices obtained in relativistic Brueckner-Hartree-Fock studies of nuclear matter.^{1,2} We require, in particular, that the self-energy of a particle in nuclear matter be reproduced correctly. Further, we also require that certain matrix elements of the quasiparticle interaction (Migdal parameters) be given correctly. As we will see, it is fairly easy to reproduce the corrections required to go from the Hartree-Fock results

for the nucleon self-energy to the results of the reaction-matrix elements. In addition, the effective interaction determined from our study of the nucleon self-energy *also* reproduces, quite well, the Migdal parameters obtained from our *G*-matrix calculations.^{1,2}

In Sec. II we review some definitions of the nucleon self-energy introduced in an earlier work^{1,2} and describe our model for the effective interaction. In Sec. III we present the results of our calculations of the nucleon self-energy and in Sec. IV we present our results for the Migdal parameters. Sec. V contains some concluding comments.

In reading the following material the reader should keep in mind that we are constructing an *effective interaction* which is to be used in the space of *Dirac spinors*. If one were to reduce this interaction to one which is effective in the space of Pauli spinors, one would obtain (in a rather direct fashion) various density-dependent effects which have their origin in the underlying relativistic description.

II. RELATIVISTIC-BRUECKNER-HARTREE-FOCK THEORY AND THE EFFECTIVE INTERACTION

We recall that the nucleon spinor in nuclear matter satisfies the Dirac equation,^{1,2}

$$[\alpha \cdot \mathbf{p} + \beta m_N + \beta \Sigma(\mathbf{p}, k_F, \{f\})]f(\mathbf{p}, s) = \epsilon(\mathbf{p})f(\mathbf{p}, s). \quad (2.1)$$

Here Σ is the self-energy which depends on the spinors $f(\mathbf{p}, s)$ and the density of the system. We found it useful to introduce various matrix elements of the self-energy.^{1,2} [These are defined in terms of a density matrix characterized by the free spinors, $u(\mathbf{p}, s)$.] We have^{1,2}

$$\Sigma_0^{++}(\mathbf{p}) = \sum_{s'} \int \frac{d\mathbf{q}}{(2\pi)^3} \frac{m_N}{E_N(\mathbf{q})} \langle \bar{u}(\mathbf{p}, s) \bar{u}(\mathbf{q}, s') | \hat{M}(1 - p_{12}) | u(\mathbf{p}, s) u(\mathbf{q}, s') \rangle \theta(k_F - |\mathbf{q}|), \quad (2.2)$$

$$\Sigma_{s's}^{+-}(\mathbf{p}) = \sum_{s''} \int \frac{d\mathbf{q}}{(2\pi)^3} \frac{m_N}{E_N(\mathbf{q})} \langle \bar{u}(\mathbf{p},s') \bar{u}(\mathbf{q},s'') | \hat{M}(1-p_{12}) | w(\mathbf{p},s) u(\mathbf{q},s'') \rangle \theta(k_F - |\mathbf{q}|) \quad (2.3)$$

$$= \langle s' | \boldsymbol{\sigma} \cdot \hat{\mathbf{p}} | s \rangle \Sigma_0^{+-}(\mathbf{p}), \quad (2.4)$$

and

$$\Sigma_0^{--}(\mathbf{p}) = \sum_{s'} \int \frac{d\mathbf{q}}{(2\pi)^3} \frac{m_N}{E_N(\mathbf{q})} \langle \bar{w}(\mathbf{p},s) \bar{u}(\mathbf{q},s') | \hat{M}(1-p_{12}) | w(\mathbf{p},s) u(\mathbf{q},s') \rangle \theta(k_F - |\mathbf{q}|), \quad (2.5)$$

etc. In these equations \hat{M} is the reaction matrix calculated in the “ladder approximation” and p_{12} is an exchange operator. The spinor $w(\mathbf{p},s)$ is equal to the spinor $v(-\mathbf{p},-s)$ defined by Bjorken and Drell.⁷ (We have suppressed reference to isospin in Eqs. (2.1)–(2.5). Note that $\Sigma^{++}(\mathbf{p})$ and $\Sigma^{--}(\mathbf{p})$, are independent of the spin index s .)

Various figures and tables appearing in Ref. 1 give the values obtained for $\Sigma_0^{++}(\mathbf{p})$, $\Sigma_0^{+-}(\mathbf{p})$, and $\Sigma_0^{--}(\mathbf{p})$ for different values of the Fermi momentum, k_F , and for two different interactions, [HEA] (Ref. 8) and [HM2] (Ref. 9). The reaction matrix M satisfies an equation of the form^{1,2}

$$\hat{M} = U + U\hat{g}\hat{M}. \quad (2.6)$$

The Hartree-Fock results for $\Sigma_0^{++}(\mathbf{p})$, $\Sigma_0^{+-}(\mathbf{p})$, and $\Sigma_0^{--}(\mathbf{p})$ are obtained by replacing \hat{M} by U in the above equations. The potential U describes the exchange of various “mesons” ($\sigma, \pi, \rho, \omega, \dots$) which play a role in the boson-exchange model of nuclear forces.

Our first goal is to find a $v_{\text{eff}} = U + \Delta U$, which when inserted into Eqs. (2.2)–(2.5), will reproduce the results obtained with the reaction matrix \hat{M} . In order to understand our model, let us look at the contribution of *sigma* exchange to certain matrix elements of the potential U :

$$\begin{aligned} \langle \mathbf{p}'_1 s'_1, \mathbf{p}'_2 s'_2 | U_{\sigma}^{++++}(1-p_{12}) | \mathbf{p}_1 s_1, \mathbf{p}_2 s_2 \rangle \\ = g_{\sigma}^2 \left[\frac{[\bar{u}(\mathbf{p}'_1 s'_1) u(\mathbf{p}_1 s_1)][\bar{u}(\mathbf{p}'_2 s'_2) u(\mathbf{p}_2 s_2)]}{q^2 - m_{\sigma}^2 + i\eta} - \frac{[\bar{u}(\mathbf{p}'_2 s'_2) u(\mathbf{p}_1 s_1)][\bar{u}(\mathbf{p}'_1 s'_1) u(\mathbf{p}_2 s_2)]}{(p_1 - p'_2)^2 - m_{\sigma}^2 + i\eta} \right]. \end{aligned} \quad (2.7)$$

Here we have again suppressed reference to isospin and the vertex cutoff (or form factors) used in the one-boson exchange (OBE) model.^{8,9} These features are included in our calculations, however.

We now define the contribution of *pseudo-sigma* exchange as follows:

$$\begin{aligned} \langle \mathbf{p}'_1 s'_1, \mathbf{p}'_2 s'_2 | \Delta U_{\sigma}^{++++}(1-p_{12}) | \mathbf{p}_1 s_1, \mathbf{p}_2 s_2 \rangle \\ = -\delta g_{\sigma}^2 \left[\frac{[\bar{u}(\mathbf{p}'_1 s'_1) u(\mathbf{p}_1 s_1)][\bar{u}(\mathbf{p}'_2 s'_2) u(\mathbf{p}_2 s_2)]}{q^2 - M_{\sigma}^2 + i\eta} - \frac{[\bar{u}(\mathbf{p}'_2 s'_2) u(\mathbf{p}_1 s_1)][\bar{u}(\mathbf{p}'_1 s'_1) u(\mathbf{p}_2 s_2)]}{(p_1 - p'_2)^2 - M_{\sigma}^2 + i\eta} \right], \end{aligned} \quad (2.8)$$

where the minus sign to the right of the equals sign can be thought of as arising from the use of an imaginary coupling constant for the pseudoparticle of mass M_{σ} . The extension of these definitions to the exchange of omega “mesons” and pseudo-omega “mesons” is straightforward.

It turns out that we only need introduce *three* pseudoparticles to reproduce various matrix elements of the reaction matrix. These are pseudo-sigma, pseudo-omega and pseudo-delta fields. For example, the potential HEA (Ref. 8) describes exchange of the following “mesons:”

σ	$J=0^+$	$T=0$
ω	$J=1^-$	$T=0$
π	$J=0^-$	$T=1$
ρ	$J=1^-$	$T=1$
δ	$J=0^+$	$T=1$
ϕ	$J=1^-$	$T=0$
η	$J=0^-$	$T=0$

One might think that a pseudo-pion would be required but (as may be seen from the figures in Ref. 1) the exchange

of pions, beyond the Born term, gives rise to effects that can be readily simulated by *sigma* exchange. Therefore, in first approximation, the role of pseudoparticle exchange is to reduce the repulsion of the omega-exchange Born terms, reduce the attraction of sigma-exchange Born terms, and to simulate the sigma-like attraction obtained from higher-order terms in the exchange of pions. As we will see, the simulation of correlation effects in pion exchange will lead to the use of a negative value for δg_{σ}^2 in Eq. (2.8), which corresponds to the use of a *real* coupling constant for the pseudosigma field.

Again, with reference to the potential HEA, we put

$$v_{\text{eff}} = v_{\text{eff}}^{(1)} + v_{\text{eff}}^{(2)}, \quad (2.9)$$

where

$$v_{\text{eff}}^{(1)} = U \quad (2.10)$$

$$= U_{\sigma} + U_{\omega} + U_{\rho} + U_{\pi} + U_{\delta} + U_{\eta} + U_{\phi}, \quad (2.11)$$

and

$$v_{\text{eff}}^{(2)} = \Delta U \quad (2.12)$$

$$= \Delta U_{\sigma} + \Delta U_{\omega} + \Delta U_{\delta} . \quad (2.13)$$

Therefore, there are six parameters (at each density) (δg_{σ}^2) , (δg_{ω}^2) , (δg_{δ}^2) , M_{σ} , M_{ω} , and M_{δ} . We fix the values of the mass parameters to be $M_{\sigma}=1.0$ GeV, $M_{\omega}=1.0$ GeV, and $M_{\delta}=1.25$ GeV, leaving only three parameters to be determined. We remark that the choice of fairly large masses for the pseudoparticles follows from the observation that the role of correlations in the calculation of Σ^{++} , for example, is to shift the magnitude of Σ^{++} without changing the momentum dependence.^{1,2} Such shifts can be obtained from a short-range interaction, that is, an interaction which arises from the exchange of a massive particle. We have not made any extensive investigation of the sensitivity of our results to modifications of the masses of the pseudoparticles.

We now describe the procedure for determining the coupling constants of the pseudoparticles. One may use the figures appearing in Ref. 1 which give the contributions of the various mesons in the calculation of the self-energy. We reproduce some of these figures in this work (see Figs. 1–8). As a specific example, let us consider the repulsion in Σ^{++} obtained from ω and ϕ exchange as shown in Fig. 2. The solid line is the Hartree-Fock result and the dashed line includes the effects of correlations. Essentially we want to choose the coupling constant of the pseudoparticles so that instead of the results shown by the solid line we get the results shown by the dashed lines. We can accomplish this by adding a pseudo-omega to the model to adjust the contribution of the ω field so that one

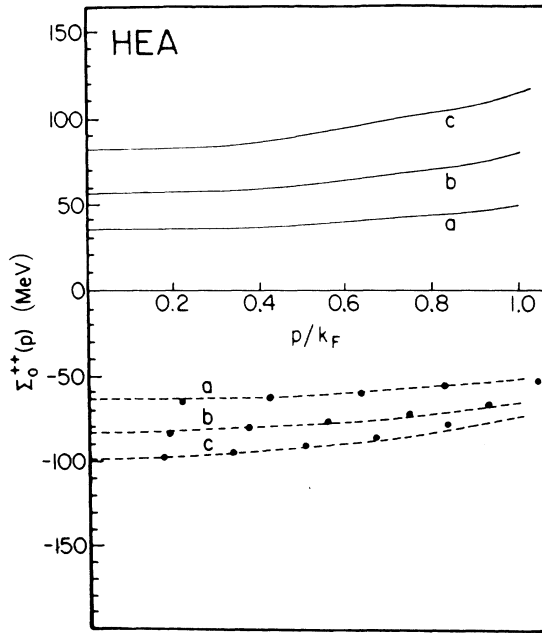


FIG. 1. The solid lines denote the Hartree-Fock results for $\Sigma_0^{++}(\mathbf{p})$ for the potential HEA and the dashed lines include the effects of correlations (Refs. 1 and 2). The solid circles in the lower half of the figure are the results obtained with v_{eff} of Eqs. (2.9)–(2.15). (a) $k_F=1.2$ fm⁻¹; (b) $k_F=1.36$ fm⁻¹; (c) $k_F=1.5$ fm⁻¹.

obtains values corresponding to the dashed lines rather than to the solid lines. The contributions of particle plus pseudoparticle exchange are denoted by the black dots. It can be seen that, with the appropriate choice of coupling constant for the pseudoparticle, the black dots can be made to fall on the dashed curve. This can also be done for the ϕ field. (If the masses of the pseudoparticles used to adjust the ω and ϕ contributions are the same, we can associate these pseudoparticle effects with the exchange of a single pseudo-omega with an appropriately modified coupling constant. This point will be discussed in more detail later in this work.)

At this point we have adjusted the ω and ϕ contributions by adding pseudo-omega particles to the model. With the coupling constants fixed from the study of Σ^{++} we can then calculate the contributions of the pseudoparticles to Σ^{+-} . With reference to Fig. 5, we note that the solid lines denote the Hartree-Fock results for σ , ω , and ϕ exchange. If we then add the contributions of pseudo-omega exchange (with the coupling constants fixed as discussed above) we obtain the black dots. Note that the black dots fall on the curves which describe the effects of correlations (dashed lines). Therefore, we see

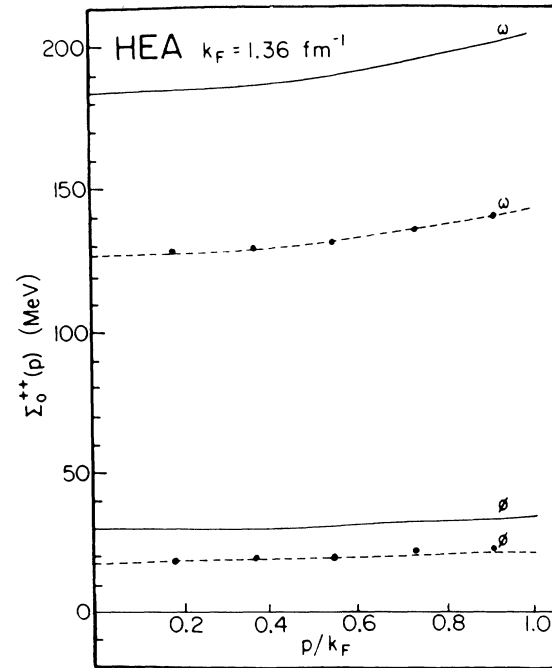


FIG. 2. The solid lines exhibit the contribution of ω and ϕ exchange to Σ_0^{++} as calculated in the Hartree-Fock approximation. The dashed lines show the contribution of ω and ϕ exchange in the presence of correlations (Ref. 1). The upper set of solid circles shows the result of omega exchange and a portion of the total pseudo-omega exchange [$(\delta g_{\omega}^2/4\pi)_1=12.30$] calculated in the Hartree-Fock approximation. The lower set of solid circles shows the similar results for phi exchange and a portion of pseudo-omega exchange [$(\delta g_{\omega}^2/4\pi)_2=1.90$]—see Table II. [Note that the total pseudo-omega exchange is calculated with $(\delta g_{\omega}^2/4\pi)=12.30+1.90=14.2$.]

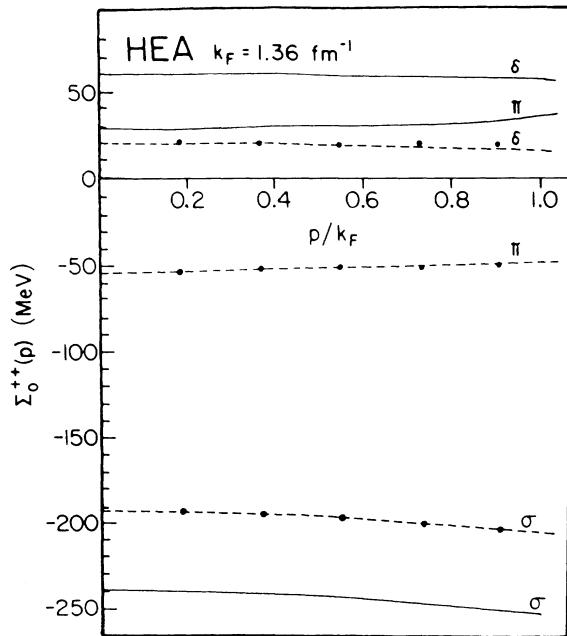


FIG. 3. The solid lines show the contributions to $\Sigma_0^{++}(\mathbf{p})$ from the exchange of σ , π , and δ "mesons" as calculated in the Hartree-Fock approximation. The dashed lines are the results for σ , π , and δ exchange in the presence of correlations (Ref. 1). The uppermost set of solid circles is the result of delta and pseudo-delta exchange ($\delta g_\delta^2/4\pi = 5.54$) calculated in the Hartree-Fock approximation. The lower set of solid circles represent sigma and pseudo-sigma exchange [$(\delta g_\sigma^2/4\pi)_1 = 3.78$ —see Table II] calculated in the Hartree-Fock approximation. In the case of the pion we add a portion of the pseudo-sigma exchange [$(\delta g_\sigma^2/4\pi)_2 = -6.59$ —see Table II] which is taken to be *attractive*. The *total* result for pseudo-sigma exchange [$\delta g_\sigma^2/4\pi = -2.81$ —see Table I] is seen to be *attractive*.

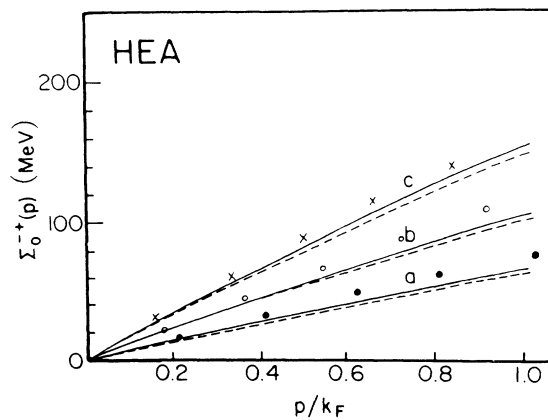


FIG. 4. The potential $\Sigma_0^{+-}(\mathbf{p})$ as obtained for the interaction HEA. The solid curves is the Hartree-Fock result and the dashed line includes the effects of correlations (see Ref. 1). The solid circles are calculated with v_{eff} of Eqs. (2.9)–(2.15). (a) $k_F = 1.2 \text{ fm}^{-1}$; (b) $k_F = 1.36 \text{ fm}^{-1}$; (c) $k_F = 1.5 \text{ fm}^{-1}$.

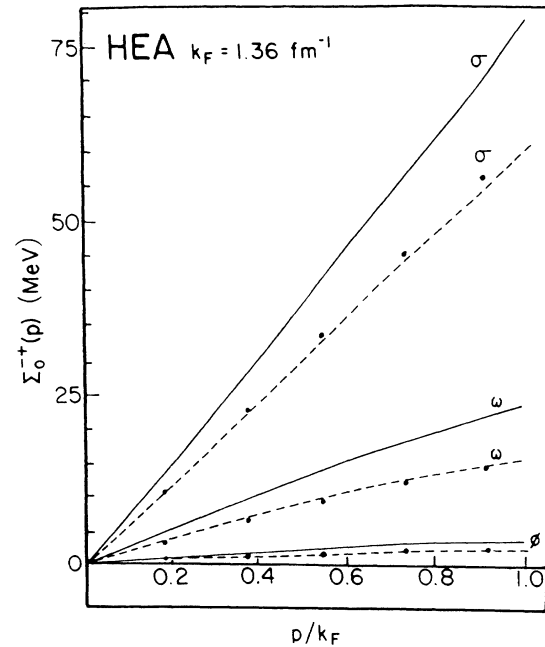


FIG. 5. The contributions of σ , ω , and ϕ exchange to $\Sigma_0^{++}(\mathbf{p})$ calculated in the Hartree-Fock approximation (solid line) and in the relativistic Brueckner-Hartree-Fock theory (dashed line) (Ref. 1). The solid circles result from adding pseudo-particle exchange to the Hartree-Fock results. [Here $(\delta g_\omega^2/4\pi)_1 = 12.30$, $(\delta g_\omega^2/4\pi)_2 = 1.90$, and $(\delta g_\sigma^2/4\pi)_1 = 3.78$ —see Table II.]

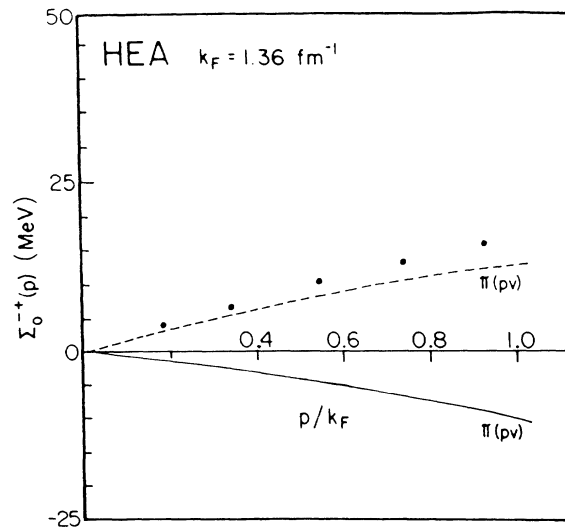


FIG. 6. The contribution of pion exchange to $\Sigma_0^{+-}(\mathbf{p})$ in the Hartree-Fock approximation (solid line) and in the relativistic Brueckner-Hartree-Fock theory (dashed line) (Ref. 1). Pseudovector coupling is used. The solid circles obtained by adding a portion of pseudo-sigma exchange with $(\delta g_\sigma^2/4\pi)_2 = -6.59$ (see Table II). Here the negative sign for $(\delta g_\sigma^2/4\pi)$ means that the contribution of the pseudo-sigma particle has the same sign as that obtained for sigma exchange.

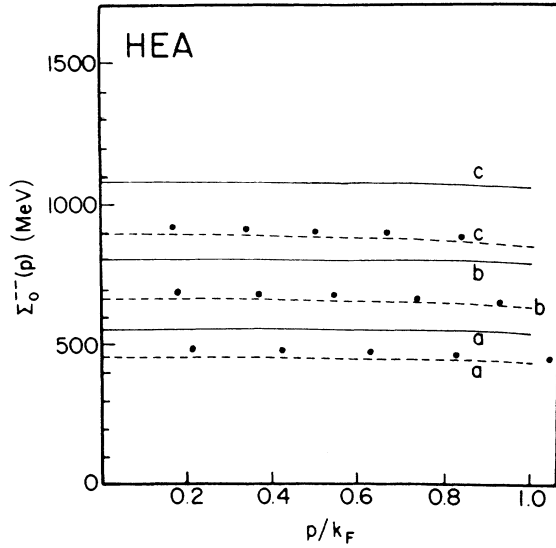


FIG. 7. The potential $\Sigma_0^-(\mathbf{p})$ calculated with the interaction HEA. The curves have the same meaning as that described in the caption of Fig. 2. Results calculated with ν_{eff} are given by solid circles.

that once we fix the pseudoparticle coupling constants from the study of Σ^{++} , no further parameter modifications are needed to adjust the contributions to Σ^{+-} . (Again, the use of a single pseudo-omega particle will adjust the summed

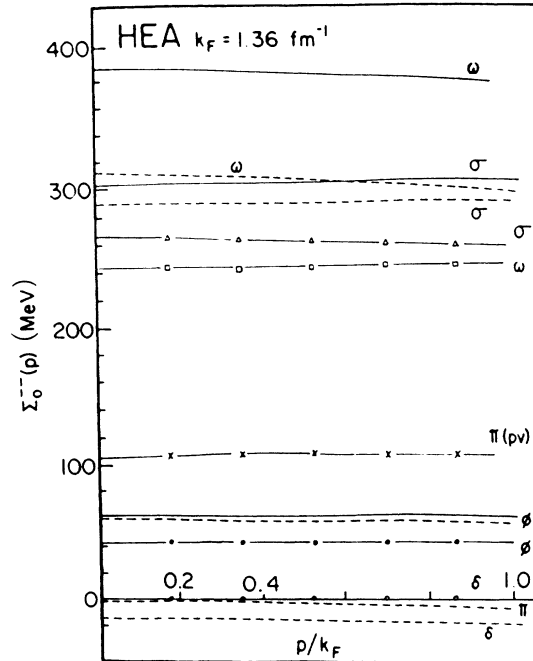


FIG. 8. The contributions of ω , σ , π , ϕ , and δ exchange to $\Sigma_0^-(\mathbf{p})$ for the potential HEA. The unbroken solid lines are the Hartree-Fock results and the dashed lines include the effect of correlations (Ref. 1). The results of calculations of meson plus pseudo-meson exchange are shown as triangles (sigma), squares (omega), crosses (pion), solid circle (phi), and open circles (delta).

contribution of the ω and ϕ fields to Σ^{+-} .)

In a similar fashion we can adjust the contributions of σ , π , and δ exchange to Σ^{++} by adding the appropriate pseudoparticles. Again, the coupling constants can be determined by studying the role of correlations in the calculation of Σ^{++} . It is then found that the situation in the case of Σ^{+-} is satisfactory (see Figs. 5 and 6).

We should note that the σ and ω fields behave quite differently in the calculation of Σ^{+-} . For example, in the Hartree approximation, the contribution of the ω field is zero, while the contribution from σ exchange is large. (The contributions of the ω field to Σ^{+-} shown in the figures come from the exchange terms of the Hartree-Fock approximation.) Therefore, while one might fix the (total) value of Σ^{++} by adding only one type of pseudoparticle, that procedure would lead to a poor fit to Σ^{+-} . On the other hand, the procedure we chose works quite well.

In summary, we can say that the coupling constants of the pseudoparticles may be adjusted to fit the contributions of the various mesons to Σ^{++} obtained in reaction-matrix calculations. It is then found that the corresponding results for Σ^{+-} are satisfactory, without the need for further modification of the coupling constants.

We have carried out our calculations at a number of different densities. It is useful to parametrize the density dependence of the various δg^2 . We write, with i denoting either pseudo-sigma, pseudo-omega, or pseudo-delta mesons, for values of $\rho/\rho_{\text{NM}} \leq 1.25$,

$$\delta g_i^2(k_F) = \delta g_i^2(k_F^{\text{NM}}) \left\{ 1 + a_1 \left[1 - \left(\frac{\rho}{\rho_{\text{NM}}} \right)^{2/3} \right] + a_2 \left[1 - \left(\frac{\rho}{\rho_{\text{NM}}} \right)^{4/3} \right] + a_3 \left[1 - \left(\frac{\rho}{\rho_{\text{NM}}} \right)^2 \right] \right\}. \quad (2.14)$$

Here $k_F^{\text{NM}} = 1.36 \text{ fm}^{-1}$ and ρ_{NM} is the density of nuclear matter. The results presented in the following are for the values

$$\begin{aligned} \delta g_\sigma^2 &= -2.81, \quad M_\sigma = 1.0 \text{ GeV}, \quad a_1 = 0.357, \\ \delta g_\omega^2 &= 14.2, \quad M_\omega = 1.0 \text{ GeV}, \quad a_2 = -0.0735, \\ \delta g_\delta^2 &= 5.54, \quad M_\delta = 1.25 \text{ GeV}, \quad a_3 = 0.00297. \end{aligned} \quad (2.15)$$

We have found other sets of δg_i^2 and a_i , however, these only differ slightly from those given above. In Table I we present the values of $\delta g_i^2(k_F)$ obtained from Eq. (2.14) and the parameters listed above.

TABLE I. The coupling constant δg_σ^2 , δg_ω^2 , and δg_δ^2 are given as a function of density (see text).

	$(1/4\pi)\delta g_\sigma^2(\rho)$	$(1/4\pi)\delta g_\omega^2(\rho)$	$(1/4\pi)\delta g_\delta^2(\rho)$
$\frac{1}{4}\rho_{\text{NM}}$	-3.25	16.42	6.40
$\frac{1}{2}\rho_{\text{NM}}$	-3.06	15.48	6.04
$\frac{3}{4}\rho_{\text{NM}}$	-2.92	14.77	5.76
ρ_{NM}	-2.81	14.20	5.54
$\frac{5}{4}\rho_{\text{NM}}$	-2.72	13.73	5.35

Note that δg_σ^2 is a negative number. With our conventions that means that the *total* pseudo-sigma exchange gives an *attractive* contribution. The reason for this will be made clear in the next section. Further, δg_ω^2 and δg_δ^2 are positive numbers, leading to attractive contributions from the exchange of these pseudoparticles. Therefore we see that all the pseudoparticle exchanges lead to attractive contributions to the mean field Σ^{++} .

III. THE NUCLEON SELF-ENERGY

In Fig. 1 we present the results obtained for $\Sigma_0^{++}(\mathbf{p})$, for various densities, for the potential HEA. The solid lines are the Hartree-Fock results and the dashed lines include the effects of correlations.^{1,2} The small dots in the lower part of the figure are based upon the use of v_{eff} [see Eqs. (2.9)–(2.15)].

It is useful at this point to consider the contribution of each meson to the calculation of $\Sigma_0^{++}(\mathbf{p})$. In Figs. 2 and 3 we show the contributions of ω , ϕ , π , σ , and δ mesons. (The contribution of the η meson is small and is not shown here.) In Figs. 2 and 3 the solid lines are the Hartree-Fock contributions at nuclear matter densities. Therefore adding these various contributions will yield the solid line labeled by the curve *b* in Fig. 1. The dashed lines in Figs. 2 and 3 are the contributions of the exchange of each meson between correlated wave functions.¹ The various solid circles in Figs. 2 and 3 are obtained as follows. The attractive contribution from pseudo-omega exchange with coupling $\delta g_\omega^2/(4\pi) = 14.20$ (see Table I) is divided into two parts, one part [$(\delta g_\omega^2/4\pi)_1 = 12.30$] ascribed to correct the result of ω exchange and another part [$(\delta g_\omega^2/4\pi)_2 = 1.90$] ascribed to correct the result of ϕ exchange—see Table II. With this choice we obtain the

results shown in Fig. 2. (Of course, it is only the summed result of both these corrections, that is relevant to the construction of Fig. 1.)

Now consider the results shown in Fig. 3. The solid circles for the δ exchange contribution reproduce the results of δ exchange in the presence of correlations (dashed line). Now consider pseudo-sigma exchange. Note that from Table I $(\delta g_\sigma^2/4\pi) = -2.81$ at nuclear matter densities. The negative sign here means that the total result for pseudo-sigma exchange is *attractive*. This can be understood from Table II and Fig. 3. As can be seen from Fig. 3, pseudo-sigma exchange is required to provide *attraction* to give the correct result for correlated pion exchange (dashed line) and *repulsion* to yield the correct result for correlated sigma exchange (dashed line.) This is accomplished by separating $(\delta g_\sigma^2/4\pi) = -2.81$ into two terms $(\delta g_\sigma^2/4\pi)_1 = 3.78$ and $(\delta g_\sigma^2/4\pi)_2 = -6.59$ as in Table II. (Formally we can consider a negative value for $\delta g^2/(4\pi)$ as arising from the exchange of the pseudoparticle with a real rather than a complex coupling constant. We can avoid confusion with respect to our choice of signs by referring to Figs. 2 and 3. There one can see whether pseudoparticle exchange yields a repulsive or attractive contribution.)

In Fig. 4 we exhibit $\Sigma_0^{+-}(\mathbf{p})$. Again the solid lines are the Hartree-Fock results and the dashed lines are the results of the reaction matrix calculations of Ref. 1. The small crosses, circles and dots are the Hartree-Fock results based upon the use of v_{eff} of Eqs. (2.9)–(2.15). Again, in Figs. 5 and 6, we show the contributions of the individual mesons. As discussed previously, we have separated pseudo-omega exchange into contributions which correct the omega and phi fields. Similarly pseudo-sigma ex-

TABLE II. Coupling constants and meson masses for the potential HEA. Also given are the coupling constants for the pseudoparticles for $k_F = k_F^{\text{NM}} = 1.36 \text{ fm}^{-1}$. (A factor of m^2/M^2 is included so that the strengths of the potentials arising from particle and pseudoparticle exchange at zero momentum transfer can be compared.)

	HEA ^a			Pseudoparticles	
	Mass (MeV)	Coupling constant ($g^2/4\pi$)	f/g	$\left[\frac{\delta g^2}{4\pi} \right]$	$\left[\frac{m^2}{M^2} \right]$
σ	500	4.63	0	$\left[\frac{\delta g_\sigma^2}{4\pi} \right]_1 = 3.78$	$\left[\frac{\delta g_\sigma^2}{4\pi} \right] \left[\frac{m_\sigma^2}{M_\sigma^2} \right] = -0.70$
π	138.5	13.0	0	$\left[\frac{\delta g_\sigma^2}{4\pi} \right]_2 = -6.59$	
ω	782.8	14.0	0	$\left[\frac{\delta g_\omega^2}{4\pi} \right]_1 = 12.30$	$\left[\frac{\delta g_\omega^2}{4\pi} \right] \left[\frac{m_\omega^2}{M_\omega^2} \right] = 8.70$
ϕ	1020	7.0	0	$\left[\frac{\delta g_\omega^2}{4\pi} \right]_2 = 1.90$	
η	548.5	6.0	0	0	
δ	960	4.74	0	$\left[\frac{\delta g_\delta^2}{4\pi} \right]_1 = 5.54$	$\left[\frac{\delta g_\delta^2}{4\pi} \right] \left[\frac{m_\delta^2}{M_\delta^2} \right] = 3.27$
ρ	763	1.50	3.5	0	

^aReference 8.

change is separated into terms which correct the sigma and pion field contribution s . The calculation is made with the coupling constants used previously and listed in Table II. It is of interest to note that the separation of the pseudoparticle exchange effects into ω and ϕ channels and σ and π channels which was made in the case of Σ^{++} also works in the case of Σ^{-+} (see Figs. 5 and 6).

In Fig. 7 we present results for $\Sigma_0^{--}(\mathbf{p})$. The small inaccuracies in the fit obtained to the dashed curves (see the solid circles, open circles, and crosses) are not significant since $\Sigma_0^{--}(\mathbf{p})$ appears as a correction to a large denominator (of the order of 2000 MeV) in the effective potential, U_{eff} , which we define below. In Fig. 8 we show the contribution of the various mesons. Again the solid lines are the results obtained using the Hartree-Fock approximation and the dashed lines are the results including correlation effects.¹ The triangles, squares, crosses, solid circles, and open circles are the result for meson plus pseudo-meson exchange for σ , ω , π , ϕ , and δ fields. Here, unlike the results obtained for Σ^{++} and Σ^{-+} , we see that the individual mesonic contributions (dashed lines) are not very well reproduced by the pseudoparticle model. However, this is not particularly important since the summed contributions reproduce Σ^{--} rather well (see Fig. 7).

We saw, in Ref. 1, that if one reduces the Dirac equation to an equivalent Schrödinger form, the effective potential has the structure

$$U_{\text{eff}}(\mathbf{p}) \simeq \frac{m_N}{E_N(\mathbf{p})} \Sigma^{++}(\mathbf{p}) + \left[\frac{m_N}{E_N(\mathbf{p})} \right]^2 \frac{\Sigma^{+-}(\mathbf{p}) \Sigma^{-+}(\mathbf{p})}{2m_N + \frac{m_N}{E_N(\mathbf{p})} [\Sigma^{++}(\mathbf{p}) - \Sigma^{--}(\mathbf{p})]} \quad (3.1)$$

for $|\mathbf{p}| \leq k_F$. More precisely, the quasiparticle energy in nuclear matter is $\epsilon(\mathbf{p}) = (\mathbf{p}^2 + m_N^2)^{1/2} + U_{\text{eff}}(\mathbf{p})$. The quantities, $\Sigma^{++}(\mathbf{p})$, $\Sigma^{+-}(\mathbf{p})$, and $\Sigma^{--}(\mathbf{p})$ differ from $\Sigma_0^{++}(\mathbf{p})$, $\Sigma_0^{+-}(\mathbf{p})$, and $\Sigma_0^{--}(\mathbf{p})$ in being defined in terms of the correct density matrix for the system, that is, the density matrix expressed in terms of the spinors $f(\mathbf{q}, s)$ —see Eq. (2.1). Note that if $\Sigma^{++}(\mathbf{p})$, $\Sigma^{+-}(\mathbf{p})$, and $\Sigma^{--}(\mathbf{p})$ are replaced by $\Sigma_0^{++}(\mathbf{p})$, $\Sigma_0^{+-}(\mathbf{p})$, and $\Sigma_0^{--}(\mathbf{p})$, one

$$\mathcal{F}(\mathbf{p}_1, \mathbf{p}_2) = \left[\frac{m_N}{E_N(\mathbf{p}_1)} \right]^{1/2} \left[\frac{m_N}{E_N(\mathbf{p}_2)} \right]^{1/2} \langle \bar{f}(\mathbf{p}_1 s'_1) \bar{f}(\mathbf{p}_2 s'_2) | \hat{M}(1 - p_{12}) | f(\mathbf{p}_1 s_1) f(\mathbf{p}_2 s_2) \rangle \left[\frac{m_N}{E_N(\mathbf{p}_1)} \right]^{1/2} \left[\frac{m_N}{E_N(\mathbf{p}_2)} \right]^{1/2}, \quad (4.1)$$

where

$$f^\dagger(\mathbf{p}, s) f(\mathbf{p}, s) = E_N(\mathbf{p}) / m_N. \quad (4.2)$$

The calculation of this amplitude is discussed in detail in Ref. 1, where an expansion of the $f(\mathbf{p}, s)$ in terms of the spinors $u(\mathbf{p}, s)$ and $w(\mathbf{p}, s)$ is used,

$$f(\mathbf{p}, s) = \frac{1}{[1 + \alpha^2(\mathbf{p})]^{1/2}} \left[u(\mathbf{p}, s) + \alpha(\mathbf{p}) \sum_{s'} \langle s' | \boldsymbol{\sigma} \cdot \hat{\mathbf{p}} | s \rangle w(\mathbf{p}, s') \right]. \quad (4.3)$$

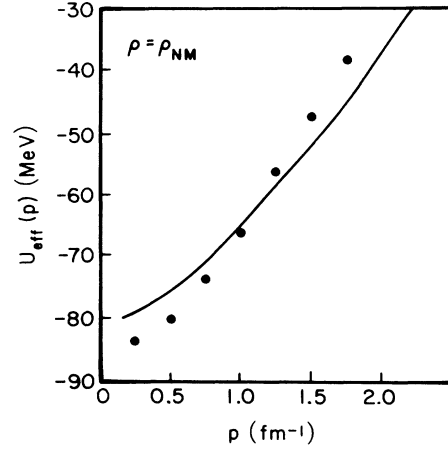


FIG. 9. The effective potential, $U_{\text{eff}}(\mathbf{p})$, calculated using the relativistic BHF theory (solid line) and the values of $U_{\text{eff}}(\mathbf{p})$ calculated using v_{eff} of Eqs. (2.9)–(2.15) are shown. Here $\rho = \rho_{\text{NM}}$.

makes only a small error in the calculation of $U_{\text{eff}}(\mathbf{p})$, and we use that approximation here.

We now proceed to present results for $U_{\text{eff}}(\mathbf{p})$, calculated using the relativistic Brueckner-Hartree-Fock (BHF) theory,¹ and compare these results with our calculations using v_{eff} of Eqs. (2.9)–(2.15). This comparison is made in Fig. 9. As can be seen from these figures, the fit is remarkably accurate for $|\mathbf{p}| < 2 \text{ fm}^{-1}$, given the simplicity of the model used to specify v_{eff} . Some of the small disagreement with the reaction matrix calculation (solid lines) is due to the fact that while we have here calculated v_{eff} using the approximation, $\Sigma^{++} \simeq \Sigma_0^{++}$, the reaction matrix calculations shown as solid lines do not include that approximation.

IV. THE MIGDAL PARAMETERS

As discussed in Refs. 1 and 2, we may obtain the Migdal parameters in the relativistic theory by considering the forward scattering amplitude for two particles of momentum \mathbf{p}_1 and \mathbf{p}_2 at the Fermi surface, that is $|\mathbf{p}_1| = |\mathbf{p}_2| = k_F$. This amplitude may be written, with $E_N(p) = (\mathbf{p}^2 + M_N^2)^{1/2}$, as

At this point we consider only the leading term,^{1,2}

$$\mathcal{F}^{\text{NR}}(\mathbf{p}_1, \mathbf{p}_2) = \left[\frac{m_N}{E_N(k_F)} \right]^{1/2} \langle \bar{u}(\mathbf{p}_1 s'_1) \bar{u}(\mathbf{p}_2 s'_2) | \hat{M}(1-p_{12}) | u(\mathbf{p}_1 s_1) u(\mathbf{p}_2 s_2) \rangle, \quad (4.4)$$

which appears in an expansion in the small parameter $\alpha(\mathbf{p})$.

We could fix the parameters of v_{eff} by requiring that the Migdal parameters calculated from the amplitude

$$\mathcal{F}_{\text{eff}}^{\text{NR}}(\mathbf{p}_1, \mathbf{p}_2) = \left[\frac{m_N}{E_N(k_F)} \right]^2 \langle \bar{u}(\mathbf{p}_1 s'_1) \bar{u}(\mathbf{p}_2 s'_2) | v_{\text{eff}}(1-p_{12}) | u(\mathbf{p}_1 s_1) u(\mathbf{p}_2 s_2) \rangle \quad (4.5)$$

are reasonably close to those obtained from $\mathcal{F}^{\text{NR}}(\mathbf{p}_1, \mathbf{p}_2)$. However, we will here calculate the Migdal parameters using the effective interaction specified in the previous sections of this work. Of course, the actual Migdal parameters of the relativistic BHF theory¹ are to be obtained using Eq. (4.1). As discussed in Ref. 1, the use of the $f(\mathbf{p}, s)$ rather than the $u(\mathbf{p}, s)$ makes major changes in the Migdal parameter F_0 . Therefore, ideally one should calculate the Migdal parameters for the amplitude

$$\mathcal{F}_{\text{eff}}(\mathbf{p}_1, \mathbf{p}_2) = \left[\frac{m_N}{E_N(k_F)} \right]^2 \langle \bar{f}(\mathbf{p}_1 s'_1) \bar{f}(\mathbf{p}_2 s'_2) | v_{\text{eff}}(1-p_{12}) | f(\mathbf{p}_1 s_1) f(\mathbf{p}_2 s_2) \rangle, \quad (4.6)$$

and compare the results with those parameters obtained for $\mathcal{F}(\mathbf{p}_1, \mathbf{p}_2)$ of Eq. (4.1). We will do that later in this section.

We will first compare the Migdal parameters obtained for the amplitudes $\mathcal{F}^{\text{NR}}(\mathbf{p}_1, \mathbf{p}_2)$ and $\mathcal{F}_{\text{eff}}^{\text{NR}}(\mathbf{p}_1, \mathbf{p}_2)$. [The Migdal parameters for $\mathcal{F}^{\text{NR}}(\mathbf{p}_1, \mathbf{p}_2)$ were given in Ref. 1 for the interactions HEA and HM2.] In Table III we present results for the Migdal parameters calculated for various values of k_F . The first line presents the results of the Hartree-Fock approximation, for the interaction $v_{\text{eff}}^{(1)} = U$. The second line gives the result for $v_{\text{eff}}^{(2)} = \Delta U$

and the third line is the result for $v_{\text{eff}} = U + \Delta U$. The fourth line gives the values of the Migdal parameters obtained from $\mathcal{F}^{\text{NR}}(\mathbf{p}_1, \mathbf{p}_2)$.^{1,2} It is to be stressed that, with a few exceptions, the interaction v_{eff} , which makes for a good fit to $\Sigma_0^{++}(\mathbf{p})$, $\Sigma_0^{+-}(\mathbf{p})$, $\Sigma_0^{-}(\mathbf{p})$, and $U_{\text{eff}}(\mathbf{p})$, leads to quite reasonable values for the Migdal parameters.

Some further details of our calculations are presented in Table IV. The first seven rows present the Hartree-Fock results for $v_{\text{eff}} = U_\pi$, $v_{\text{eff}} = U_\eta$, $v_{\text{eff}} = U_\sigma$, etc. The result for $v_{\text{eff}} = U$ is then given in the eighth row. (We note that there is a great deal of cancellation among the various

TABLE III. Migdal parameters for the potential HEA calculated for the case where the nucleon spinor is $u(\mathbf{p}, s)$ with $|\mathbf{p}| = k_F$ (see text). The first line is the Hartree-Fock result ($v_{\text{eff}} = U$), the second line is calculated with $v_{\text{eff}} = \Delta U$, and the third line is the result obtained for $v_{\text{eff}} = U + \Delta U$. The fourth line is a result of a reaction matrix calculation. (Note that the Migdal parameters given here are not those of the relativistic BHF theory.)

k_F (fm ⁻¹)	F_0	F_1	F'_0	F'_1	G_0	G_1	G'_0	G'_1
1.36	3.387	-1.657	-3.168	0.197	0.895	0.516	-0.377	0.026
	-5.462	0.335	3.455	0.308	-0.443	0.062	1.425	0.282
	-2.330	-1.197	0.527	0.490	0.386	0.539	1.077	0.306
	-2.095	-1.251	0.551	0.539	0.365	0.511	1.178	0.246
1.00	1.985	-0.936	-2.275	0.221	0.876	0.356	-0.213	0.054
	-4.507	0.169	3.052	0.164	-0.365	0.039	1.306	0.148
	-2.607	-0.728	0.827	0.376	0.473	0.382	1.100	0.200
	-2.439	-0.841	0.897	0.475	0.362	0.349	1.097	0.190
1.20	2.707	-1.311	-2.778	0.225	0.891	0.452	-0.311	0.050
	-5.090	0.256	3.323	0.243	-0.413	0.051	1.394	0.220
	-2.544	-0.976	0.712	0.454	0.426	0.478	1.144	0.267
	-2.266	-1.069	0.694	0.534	0.370	0.441	1.140	0.231
1.40	3.568	-1.749	-3.262	0.186	0.895	0.533	-0.391	0.019
	-5.543	0.356	3.478	0.324	-0.449	0.064	1.428	0.298
	-2.259	-1.252	0.477	0.496	0.375	0.554	1.068	0.314
	-2.046	-1.302	0.517	0.538	0.363	0.526	1.187	0.249
1.60	4.537	-2.244	-3.719	0.100	0.879	0.596	-0.465	-0.043
	-5.903	0.461	3.555	0.402	-0.472	0.074	1.432	0.377
	-1.827	-1.555	0.216	0.493	0.318	0.610	1.005	0.340
	-1.756	-1.592	0.361	0.529	0.348	0.583	1.235	0.255

TABLE IV. Various contributions to the Migdal parameters. The first seven rows give the contribution of the Born terms for each of the mesons indicated. The contributions from pseudoparticle exchange (ΔU_σ , ΔU_ω , and ΔU_δ) are given as well as their sum (ΔU). The total is the result for $v_{\text{eff}}=U+\Delta U$ and is compared to reaction matrix results of Ref. 1. Here $k_F=1.36\text{ fm}^{-1}$ (see caption to Table III).

	F_0	F_1	F'_0	F'_1	G_0	G_1	G'_0	G'_1
U_η	0.068	-0.050	0.068	-0.050	-0.023	0.017	-0.023	0.017
U_π	1.234	-0.266	-0.411	0.089	-0.411	0.089	0.137	-0.030
U_σ	-9.211	0.732	1.773	0.732	1.773	0.732	1.773	0.732
U_δ	1.928	0.326	-3.693	-0.109	1.928	0.326	-0.643	-0.109
U_ω	7.558	-1.261	-1.352	-0.588	-1.537	-0.536	-1.537	-0.536
U_ρ	0.347	-0.818	0.922	0.194	-0.634	-0.076	0.212	0.025
U_ϕ	1.208	-0.195	-0.235	-0.086	-0.267	-0.075	-0.267	-0.075
Sum	3.132	-1.532	-2.928	0.182	0.829	0.477	-0.348	0.024
ΔU_σ	-1.312	0.056	0.354	0.056	0.354	0.056	0.354	0.056
ΔU_ω	-2.749	0.444	0.531	0.197	0.604	0.171	0.604	0.171
ΔU_δ	-1.401	-0.165	2.570	0.055	-1.401	-0.165	0.467	0.055
ΔU	-5.462	0.335	3.455	0.308	-0.443	0.062	1.425	0.282
$v_{\text{eff}}=U+\Delta U$	-2.330	-1.197	0.527	0.490	0.386	0.539	1.077	0.306
G matrix results	-2.095	-1.251	0.551	0.539	0.365	0.511	1.178	0.246
Error (%)	11.22	4.32	4.36	9.09	5.75	5.48	8.57	24.39

contributions to each Migdal parameter.) In the next three rows we have the contributions from $v_{\text{eff}}=\Delta U_\sigma$, $v_{\text{eff}}=\Delta U_\omega$, and $v_{\text{eff}}=\Delta U_\delta$. The sum of these contributions, that is, the result for $v_{\text{eff}}=\Delta U$ is given as ΔU . Finally, the result for $v_{\text{eff}}=U+\Delta U$ is given. That result is then to be compared to the result of reaction matrix calcu-

lations. The last row gives the percentage error seen in this comparison. On the whole, given the large amount of cancellation in these sums, the result obtained is quite good. We again stress that these Migdal parameters are *not* those of the fully self-consistent RBHF theory.

We now turn to the comparison of $\mathcal{F}_{\text{eff}}(\mathbf{p}_1, \mathbf{p}_2)$ and

TABLE V. Migdal parameters for the potential HEA calculated for the case where the nucleon spinor is $f(\mathbf{p}, s)$ with $|\mathbf{p}|=k_F$ (see text). The first line is the Hartree-Fock result ($v_{\text{eff}}=U$); the second line is calculated with $v_{\text{eff}}=\Delta U$ and the third line is the result obtained for $v_{\text{eff}}=U+\Delta U$. The fourth line is the result of a reaction matrix calculation. (Note that the Migdal parameters given here are those of the relativistic BHF theory.)

k_F (fm $^{-1}$)	F_0	F_1	F'_0	F'_1	G_0	G_1	G'_0	G'_1
1.36	4.440	-2.861	-2.386	-0.044	0.783	0.206	-0.387	-0.055
	-5.349	0.729	3.088	0.288	-0.407	0.116	1.364	0.231
	-0.909	-2.132	0.702	0.244	0.376	0.382	0.977	0.176
	-0.904	-1.992	0.634	0.358	0.381	0.423	1.051	0.223
1.00	2.070	-1.094	-2.109	0.178	0.817	0.310	-0.225	0.041
	-4.490	0.228	2.944	0.165	-0.359	0.045	1.296	0.140
	-2.420	-0.866	0.885	0.343	0.458	0.355	1.071	0.181
	-2.236	-0.971	0.900	0.446	0.364	0.336	1.074	0.188
1.20	3.161	-1.857	-2.371	0.104	0.818	0.323	-0.312	0.010
	-5.040	0.443	3.147	0.237	-0.398	0.076	1.365	0.196
	-1.879	-1.414	0.776	0.341	0.420	0.399	1.053	0.206
	-1.705	-1.424	0.723	0.450	0.376	0.401	1.080	0.222
1.40	4.816	-3.167	-2.360	-0.092	0.771	0.241	-0.405	-0.076
	-5.410	0.814	3.051	0.296	-0.407	0.127	1.357	0.236
	-0.594	-2.353	0.691	0.204	0.364	0.368	0.952	0.160
	-0.613	-2.187	0.622	0.319	0.382	0.419	1.034	0.219
1.60	7.376	-5.392	-1.868	-0.467	0.669	0.005	-0.510	-0.244
	-5.592	1.431	2.651	0.317	-0.385	0.206	1.274	0.239
	1.784	-3.961	0.783	-0.150	0.284	0.211	0.764	-0.005
	1.865	-3.737	0.690	-0.036	0.392	0.298	0.828	1.159

TABLE VI. Various contributions to the Migdal parameters. The first seven rows give the contribution of the Born terms for each of the mesons indicated. The contributions from pseudoparticle exchange (ΔU_σ , ΔU_ω , and ΔU_δ) are given as well as their sum (ΔU). The total is the result for $v_{\text{eff}} = U + \Delta U$ and is compared to reaction matrix results of Ref. 1. Here $k_F = 1.36 \text{ fm}^{-1}$ (see caption to Table III).

	F_0	F_1	F'_0	F'_1	G_0	G_1	G'_0	G'_1
U_η	0.062	-0.045	0.062	-0.045	-0.021	0.015	-0.021	0.015
U_π	1.109	-0.239	-0.370	0.080	-0.370	0.080	0.123	-0.027
U_σ	-8.194	0.602	1.673	0.602	1.673	0.602	1.673	0.602
U_δ	1.826	0.212	-3.349	-0.071	1.826	0.212	-0.609	-0.071
U_ω	7.836	-2.147	-1.073	-0.637	-1.488	-0.519	-1.488	-0.519
U_ρ	0.544	-0.902	0.856	0.125	-0.579	-0.052	0.193	0.017
U_ϕ	1.257	-0.342	-0.185	-0.098	-0.258	-0.072	-0.258	-0.072
Sum	4.400	-2.861	-2.386	-0.044	0.783	0.266	-0.387	-0.055
ΔU_σ	-1.161	0.036	0.336	0.036	0.336	0.036	0.336	0.036
ΔU_ω	-2.860	0.779	0.420	0.223	0.585	0.166	0.585	0.166
ΔU_δ	-1.328	-0.086	2.332	0.029	-1.328	-0.086	0.443	0.029
ΔU	-5.349	0.729	3.088	0.288	-0.407	0.116	1.364	0.231
$v_{\text{eff}} = U + \Delta U$	-0.909	-2.132	0.702	0.244	0.376	0.382	0.977	0.176
G matrix results	-0.904	-1.992	0.634	0.358	0.381	0.423	1.051	0.223
Error (%)	0.55	7.03	10.73	31.84	1.31	9.69	7.04	21.07

$\mathcal{F}(\mathbf{p}_1, \mathbf{p}_2)$ of Eqs. (4.5) and (4.1). The Migdal parameters obtained from the amplitude $\mathcal{F}(\mathbf{p}_1, \mathbf{p}_2)$ have already been given in Ref. 1. We may calculate $\mathcal{F}_{\text{eff}}(\mathbf{p}_1, \mathbf{p}_2)$ using the following expression for $f(\mathbf{p}, s)$,

$$f(\mathbf{p}, s) = \left[\frac{E_N(\mathbf{p})}{m_N} \frac{\tilde{m}}{\tilde{E}(\mathbf{p})} \right]^{1/2} \left[\frac{\tilde{E}(\mathbf{p}) + \tilde{m}}{2\tilde{m}} \right]^{1/2} \times \left[\frac{\chi_s}{\tilde{E}(\mathbf{p}) + \tilde{m}} \frac{\boldsymbol{\sigma} \cdot \mathbf{p}}{\tilde{E}(\mathbf{p}) + \tilde{m}} \chi_s \right] \quad (4.7)$$

$$= \left[\frac{E_N(\mathbf{p})}{m_N} \frac{\tilde{m}}{\tilde{E}(\mathbf{p})} \right]^{1/2} u(\mathbf{p}, s, \tilde{m}), \quad (4.8)$$

where $\tilde{m} = m_N + \frac{1}{4} \text{Tr} \Sigma(\mathbf{p})$ and $\tilde{E}(\mathbf{p}) = (\mathbf{p}^2 + \tilde{m}^2)^{1/2}$. Note that the spinor

$$\phi(\mathbf{p}, s) \equiv \left[\frac{m_N}{E_N(\mathbf{p})} \right]^{1/2} f(\mathbf{p}, s) \quad (4.9)$$

satisfies the normalization condition

$$\phi^\dagger(\mathbf{p}, s) \phi(\mathbf{p}, s) = 1. \quad (4.10)$$

When using Eq. (4.7) we can usually neglect the rather weak momentum dependence of $\tilde{m}(\mathbf{p})$, however, we have kept the density dependence of this quantity in our calculations. Note that if we put¹

$$\Sigma(\mathbf{p}) = A(\mathbf{p}) + B(\mathbf{p})\gamma^0 + \frac{\boldsymbol{\gamma} \cdot \mathbf{p}}{m_N} C(\mathbf{p}), \quad (4.11)$$

we have

$$\tilde{m}(\mathbf{p}) = m_N + A(\mathbf{p}). \quad (4.12)$$

For the calculation of the Migdal parameters, we should

use $\tilde{m} = \tilde{m}(k_F)$ in Eq. (4.7) since we are dealing with particles at the Fermi surface. As we have seen in Ref. 1, the result for F_0 is particularly sensitive to the details of the calculation, since this quantity goes through zero at some density slightly above that of nuclear matter.

In Table V we present our results for the Migdal parameters of the RBHF model. We see from this table that our effective interaction does a good job in reproducing the Migdal parameters obtained from the full G -matrix analysis. As has been noted previously, the relativistic theory gives a value of $F_0 > -1.0$ at $k_F = 1.36 \text{ fm}^{-1}$, which is necessary if the system is to have a positive compressibility parameter at nuclear matter densities.

In Table VI we present details of our calculation. This material is similar to that presented in Table IV except that we are now using the spinors $f(\mathbf{p}, s)$ instead of the $u(\mathbf{p}, s)$ [see Eqs. (4.1)–(4.10)]. We also provide, in Table VII the values of $A(k_F)$ and $\tilde{m}(k_F) = m_N + A(k_F)$ used to generate the numbers given in Table VI.

V. SUMMARY

The original Brueckner program required that one calculate the properties of nuclear matter and finite nuclei

TABLE VII. Values of $A(k_F)$ and $\tilde{m}(k_F)$ used to calculate the Migdal parameters of Table VI ($k_F = 1.36 \text{ fm}^{-1}$). Values of the parameters to be used at other densities are also shown.

k_F (fm ⁻¹)	A (MeV)	\tilde{m} (fm ⁻¹)	$[\tilde{m}(k_F)/\tilde{E}(k_F)]^{1/2}$
1.6	-480	2.325	0.908
1.4	-365	2.908	0.949
1.36	-345	3.010	0.955
1.2	-255	3.466	0.972
1.0	-151	3.993	0.985

starting from the knowledge of the nucleon-nucleon interaction in free space. The use of the Dirac equation for the description of nucleon motion has led to important advances in this program. However, calculations of the properties of finite nuclei are very difficult unless one uses the Dirac-Hartree or Dirac-Hartree-Fock approximation. In this work we have determined a (density-dependent) effective interaction which reproduces a number of properties of the nuclear-matter reaction matrix. This interaction may be used in Dirac-Hartree-Fock studies of the structure of finite nuclei. These studies may now be carried forward without the introduction of free parameters.

In a future work we will discuss the calculation of nuclear matter saturation curves for the model described here. We will also discuss such curves for a modified pseudoparticle model where we neglect the density dependence of the pseudoparticle coupling constants.

ACKNOWLEDGMENTS

This work was supported in part by the National Science Foundation and the City University of New York (PSC-BHE) Faculty Research Award Program.

¹M. R. Anastasio, L. S. Celenza, W. S. Pong, and C. M. Shakin, Phys. Rep. **100**, 327 (1983).

²L. S. Celenza and C. M. Shakin, *Relativistic Nuclear Physics: Theories of Structure and Scattering* (World Scientific, Singapore, 1986).

³B. D. Serot and J. D. Walecka, in *Advances in Nuclear Physics*, edited by J. Negele and E. Vogt (Plenum, New York, 1985), Vol. 16.

⁴B. C. Clark, S. Hama, R. L. Mercer, L. Ray, and B. D. Serot, Phys. Rev. Lett. **50**, 1644 (1983); J. R. Shepard, J. A. McNeil,

and S. J. Wallace, *ibid.* **50**, 1443 (1983); J. A. McNeil, J. R. Shepard, and S. J. Wallace, *ibid.* **50**, 1439 (1983).

⁵C. J. Horowitz and B. D. Serot, Nucl. Phys. **A368**, 503 (1981).

⁶A. Bouyssy, J. F. Mathiot, Nguyen Van Giai, and S. Marcos, Report No. IPNO/TH 86-27, 1986.

⁷J. D. Bjorken and S. D. Drell, *Relativistic Quantum Mechanics* (McGraw-Hill, New York, 1964).

⁸K. Holinde, K. Erkelenz, and R. Alzetta, Nucl. Phys. **A198**, 598 (1972).

⁹K. Holinde and R. Machleidt, Nucl. Phys. **A256**, 479 (1976).